Carbon Fibre Reinforced Polymer Composite Retrofitted Steel Profiles Using Automated Fibre Placement

Ebrahim Oromiehie, Feleb Matti, Fidelis Mashiri, and Gangadhara B. Prusty

Abstract Traditional methods for repairing impaired structures such as concreting, steel jackets, or timber splicing are impractical because of the inherent constraints associated with these materials. They would be susceptible to the same deterioration as the existing structure, leading to an ongoing cycle of repairs. Fibre-reinforced polymer (FRP) composite jackets offer a wide range of advantages including superior corrosion resistance, lightweight properties, and long-lasting durability. These characteristics make FRP composite jackets highly advantageous compared to conventional repair systems. Additionally, they can be effectively utilized for repairing various types of structures, including those made of timber, steel, and concrete. FRP composite jackets can be implemented through several techniques. However, in the experimental investigation presented in this chapter, automated fibre placement (AFP) was used to overwrap and reinforce two sets of thin-walled square hollow sections (SHS), columns and beams, with thermoplastic carbon fibre reinforced polymer (CFRP). The results obtained were then compared with the control samples without CFRP reinforcement. For the control columns, a good agreement was observed between the predicted and experimental ultimate compressive loads. The ultimate loads of CFRP reinforced columns exceeded the ultimate loads of the control columns. Inward and outward buckling was observed in each column. Debonding, tearing, and snapping of the CFRP plies was observed in column specimens with thermoplastic CFRP reinforcement. For the control beams, there was a comparable agreement between the predicted ultimate load and the experimental ultimate load. It was found that the ultimate loads for some strengthened beams were higher

E. Oromiehie (✉) · G. B. Prusty
ARC Training Centre for Automated Manufacture of Advanced Composites (AMAC), School of Mechanical and Manufacturing Engineering, UNSW Sydney, Kensington, NSW 2052, Australia
e-mail: e.oromiehie@unsw.edu.au

G. B. Prusty
Sovereign Manufacturing Automation for Composites CRC Ltd. (SOMAC CRC), Sydney, NSW, Australia

F. Matti · F. Mashiri
School of Engineering, Design and Built Environment, Western Sydney University, Penrith, NSW 2751, Australia

S. B. Singh and C. V. R. Murty (eds.), *RC Structures Strengthened with FRP for Earthquake Resistance*, Composites Science and Technology,
https://doi.org/10.1007/978-981-97-0102-5_3

than that of the control beams. For all beams, there was inward deformation on the upper surface of each beam, and outward deformations were observed on the two side walls of the SHS beams. This experimental investigation showed that the current strengthening processes using AFP is not comparable to traditional CFRP strengthening methods which use epoxy and FRP plies and that further research is required in this space. Due to the failure modes observed, future research is planned to improve the reinforcement method using AFP. The planned improvements are surface preparation, AFP processing conditions, number of CFRP layers and orientation of the CFRP.

Keywords Automated fibre placement · Thermoplastic composites · Steel beam retrofitting · Fibre reinforced polymer jackets

1 Introduction

1.1 Retrofitting in Construction

Retrofitting the critical component of structures has become more vital in the progress of civil engineering in present days. This involves the process of strengthening existing structures, both in the short and long-term, through the addition of new materials to protect them from natural events such as flooding, earthquakes, and high winds as well as maintenance of structural cracks and damages, correction of errors in design or construction, ensuring the security and the safety of the structure, reconstructing the structure for the advantages of excessive loading, etc. Retrofitting is mainly used for changing, repairing, and modifying the structures after they have been constructed [1]. In the construction industry, retrofitting is classified into global and local with subclassifications [2] which are depicted in Fig. 1.

1.1.1 Jacketing Methods

The focus of this chapter is on the local jacketing method for steel structures/profiles that are mainly used in civil structures. This technique is employed to enhance the ability of concrete, steel, and timber structures to bear heavier loads when the structural members lack sufficient capacity and also to safeguard them from further deterioration [3]. In general, jacketing is classified into (a) reinforced concrete jacketing, (b) steel jacketing, and (c) fibre reinforced polymer composite jacketing.

Reinforced Concrete Jacket (RCJ)

To reinforce concrete elements in buildings, retrofitting methods are employed on structural elements such as walls, columns, and beams using various combinations such as surface, web and flange strengthening. They aim to improve the axial and

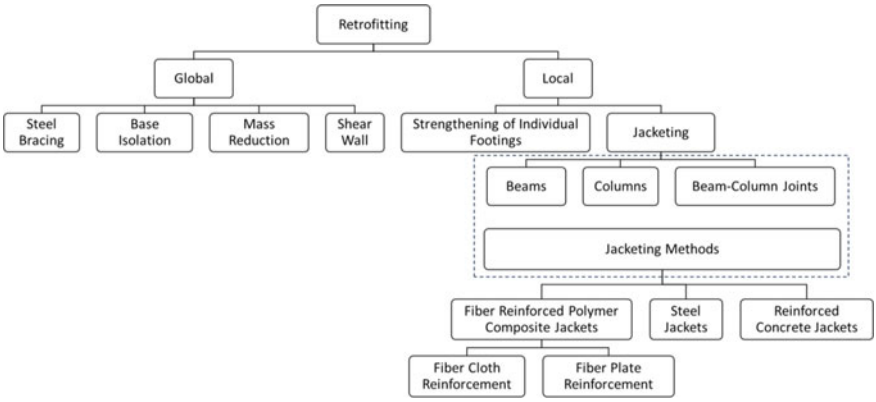

Fig. 1 Retrofitting classification

shear strength of columns while minimizing the need for extensive foundation reinforcement. In this retrofitting technique for reinforced cement concrete (RCC) buildings a cage-like structure made from steel reinforcement, or a composite material wrap is constructed around the deteriorated section. This cage serves as a foundation onto which cast-in-place concrete or shotcrete is applied. Jacketing is also effective for repairing collapsed columns, piers, and piles can even be utilized in underwater applications [2–4].

Steel Jacket (SJ):

The steel jacketing reinforcement technique involves wrapping section steel, typically angle steel, around the corners of a structural member to enhance the load-bearing capabilities, ductility, and rigidity of the component without altering its size, resulting in more reliable structural performance. It is particularly suitable for reinforcing structures where increasing the cross-sectional size of the original member is not feasible but a substantial boost in load-bearing capacity, ductility, and rigidity is required. The steel jacketing technique requires applying structural adhesive to affix steel onto the reinforced component, creating a unified and integrated system. This method is suitable for strengthening structures where enlarging the original member's cross-sectional size is not possible, but there is a significant need to enhance the cross-section's load-bearing capacity, as well as improve ductility and rigidity. The main advantages of steel jacketing include its simplicity, ease of construction, ability to significantly enhance the load-carrying capacity of the structure, low onsite workload, and short construction time [2–5].

Fibre Reinforced Polymer Composite Jacket (FRPCJ):

FRP composite jackets, provide enhanced characteristics like corrosion resistance, lightweight, and durability, which make them superior to traditional repair systems. They are also compatible with steel, concrete, and timber structures.

Fibre reinforced polymer composite (FRPC) jacketing is classified into fibre cloth reinforcement and fibre plate reinforcement technology, which are relatively new for repair and reinforcement of structures. This method involves using resin bonding materials to adhere fibre-reinforced polymer (FRP) products onto the surfaces of the building components that are expected to experience high stress. The main advantages of FRPC jacketing are listed below [2, 3, 6],

- Provide a distinct reinforcing effect on the narrow working surface because of their flexibility and ability to be wrapped around structures.
- Lightweight yet high-strength, resulting in minimal changes to the weight and appearance of the reinforced structure. Additionally, their low thickness has a negligible impact on shear moment.
- The construction process is quick and efficient.
- Carbon fibres with their high elastic modulus, offer improved control over factors such as temperature, cracks, and expansion due to rust after reinforcement.
- The original structure remains undamaged as no fasteners such as bolts, anchors, or external compression are necessary.
- Reduced manpower, materials, and construction time [4].

The effectiveness of an FRP jacket system is influenced primarily by three material parameters: thickness, fibre type, and fibre orientation. The thickness of the FRP jacket plays a significant role in the strength and ductility of repaired columns. It is directly related to the confinement pressure exerted by the FRP jacket, with higher thickness leading to increased confinement effectiveness [7, 8].

FRP wraps with higher thickness significantly enhance the strength and ductility of wrapped concrete columns [9]. The same effect is observed in both steel and timber structures since the exerted confining pressure is the crucial factor [10]. Nevertheless, for hollow steel tubes, once the jacket thickness reaches a specific threshold, where the dominant behaviour becomes inward buckling deformation of the jacket, further increasing the jacket thickness does not provide significant additional benefit as the jacket's resistance to inward buckling deformation is limited [11]. There is also a limitation on the thickness of a multilayer FRP laminate strengthening system due to the increased potential failure modes introduced by additional layers. Failure can occur in the adhesive between each layer, increasing the risk of failure within the FRP. For example, two layers for pultruded plates and three layers for FRP fabrics [12].

The magnitude of the confining stress applied by the prefabricated FRP jacket is the main factor influencing the effectiveness of the repair system and is highly influenced by the type and orientation of the fibres, regardless of the core material (concrete, steel, or timber) [13, 14]. Glass fibres are more cost-effective than carbon fibres. However, carbon fibres exhibit superior characteristics. Aramid fibres, on the other hand, have lower compressive load capacities compared to other fibres [15]. However, in prefabricated FRP jackets, fibres are oriented in the circumferential direction, in order to produce higher lateral stresses. This will result in an increased axial load capacity. Also, additional fibres with various angles relative to the hoop and longitudinal directions are used to provide resistance against multi-axial strains,

enhance the structural integrity of the entire FRP shell, and exhibit more ductile behaviour upon failure [16]. Finally, increasing the confining pressure significantly increases the ductility enhancement ratio [7, 17].

1.2 Reinforcement Techniques

1.2.1 Wet Lay-Up

The wet layup process involves grinding the surface of a column or structure and applying resin to the surface. This is followed by layering on reinforcing fibre and using a roller to impregnate the fibres with resin and compact the layers. Proper application and impregnation of the reinforcement is essential for effective FRP strengthening, as it ensures the transfer of tangential stress from the existing structural member to the FRP retrofitting. Additionally, an external resin layer contributes to the impregnation of the fabric while providing protection to the fibres against potentially harmful environments, such as marine environments. The wet lay-up method is commonly employed in the production of large structures such as ship hulls. Historically, it has been a dominant manufacturing technique due to its low initial setup and tooling costs, as well as the relatively low skill level required for component manufacturing [18]. It is a labor-intensive process that involves applying each layer and ensuring proper wetting of the fibre reinforcement. This approach has several limitations, resulting in highly inconsistent components in terms of weight, fibre volume fraction, and strength. To mitigate these variations and minimize excess resin, vacuum bagging is commonly employed in conjunction with the wet layup procedure [6, 19].

1.2.2 Interposition of a Separating Film (ISF)

The ISF technique involves the use of a polymer film placed between the column and the FRP. This method prevents the substrate from being wetted by the thermosetting matrix, thereby avoiding irreversible permanent bonding. It is particularly suitable for confinement applications where the interaction is based on contact rather than bond. In cases of confinement, the FRP is activated passively by the lateral deformation of the material, generating stress in the FRP jacket in the hoop direction. In this scenario, the contact between the substrate and the confinement jacket remains intact until either the fibres rupture or adhesion is lost in the overlap region. For successful implementation of the ISF technique, the interposed polymer film should possess several characteristics, including low roughness to minimize friction between the FRP and the substrate, thereby facilitating potential future removal of the retrofitting. Also, it should exhibit low stiffness to simplify and expedite installation. Moreover, the film should be resistant to the heat generated by the exothermic crosslinking

reaction of the epoxy matrix and be cost-effective to avoid significant cost increases in interventions that already involve expensive materials like carbon fibre [20].

1.2.3 Liquid Adhesion Release-Agent (LAR)

This method involves applying an inhibitor to the masonry surface. The objective is to create a transparent and protective layer that prevents adhesion between the epoxy matrix of the FRP and the masonry. When implementing the LAR technique, it is essential to choose a suitable adhesion-inhibiting material that ensures the detachment of the resin matrix without causing chemical alterations (maintaining breathability) or aesthetic changes (chromaticity) to the substrate. Adhesion between two materials can be primarily categorized as either chemical or mechanical. Chemical adhesion involves various types of bonds such as pure or polar primary covalent bonds, metallic, ionic, polar (or hydrogen) bonds, and Van der Waals forces. On the other hand, mechanical adhesion relies on the surface roughness, enabling one material to grip onto another. The LAR technique belongs to chemical adhesion. The primary chemical adhesion mechanism when using epoxy resin (e.g., for FRP) is hydrogen bonding. Liquid release agents, which exhibit water repellent properties, are employed to prevent hydrogen bonding. Additionally, these materials also serve as protectors for the masonry substrate, safeguarding it from weathering effects [20].

1.2.4 Filament Winding (FW)

In FW, fibre tows are impregnated with resin prior to being wrapped around a rotating mandrel. This process is commonly employed for cylindrical and spherical components, such as pipes and pressure vessels. The winding process is inherently automated, enabling cost-effective production of consistent components. This method is constrained to tubular parts and is not suitable for manufacturing open structures. Nevertheless, with a sufficiently flexible machine, it can be adapted to produce slightly more complex shapes. One challenge is achieving uniform fibre distribution and resin content across the entire thickness of the laminate. The filament winding process demonstrates excellent repeatability, making it a cost-effective choice. By maintaining a fibre to matrix volume fraction of 60:40. This technique can produce components with relatively high strength. An additional advantage of this process is the enhanced torsional strength it imparts to the final beam [18, 20].

1.2.5 Pultrusion

This is a fully automated method for producing composite materials. It is commonly employed to create fibre-reinforced sections with diverse shapes and sizes. This process is widely available and predominantly utilized in the civil engineering sector.

Its primary purpose is to fabricate composite components with a consistent cross-section. In this method, tows or fabric are saturated with resin and then passed through a heated die for curing. Additionally, resin can be directly injected into the die during the process. Pultrusion stands out as the most efficient composite manufacturing technique, boasting high productivity when compared to other methods. However, a limitation of this approach is that the fibres tend to be oriented primarily in the longitudinal direction of the beam element [18].

1.2.6 Automated Fibre Placement (AFP)

Automated fibre placement (AFP) is a high-speed manufacturing process that combines the laying, curing/melting, and consolidation steps into a single apparatus. This integration significantly improves the efficiency and output of this approach [21–23]. The AFP machine comprises of a placement head and a robotic arm, both of which are controlled by advanced software packages, Fig. 2 [24, 25].

During a lay-up, the placement head brings the surfaces of the prepreg tape together under heat and pressure to form the bonding. To apply this pressure and eliminate air from the composite structure, a consolidation roller is utilized, while a

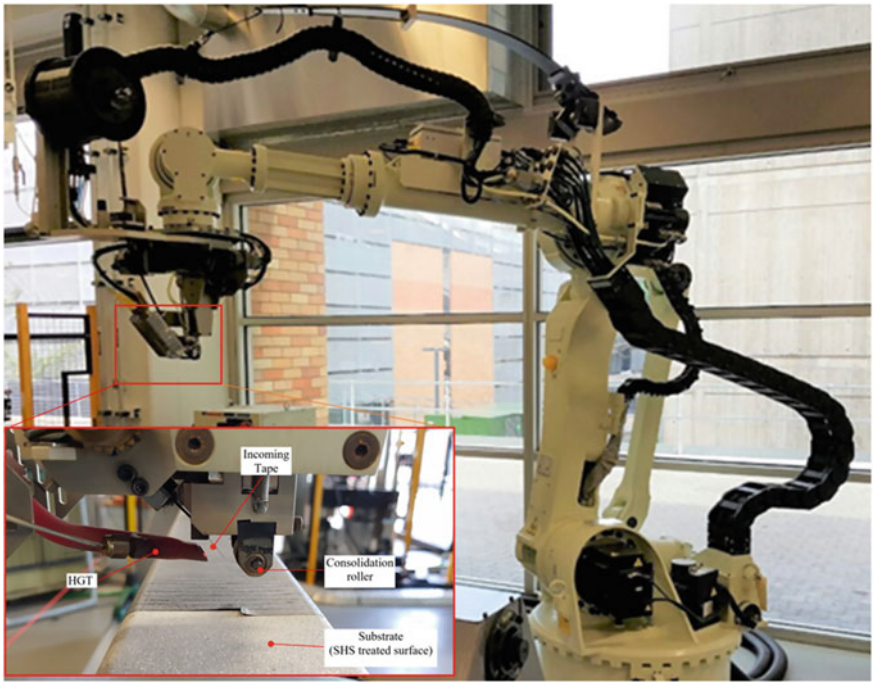

Fig. 2 Automated fibre placement (AFP) machine with thermoplastic head. *Photo courtesy* UNSW Sydney

heat source such as a hot gas torch (HGT) or laser system is employed. The cooling process is done at room temperature. The quality of the end product is influenced by various factors such as temperature, pressure, and the deposition rate of materials. Hence, it is important to ensure that these factors remain within the allowed limits or tolerances to maintain the desired quality [25]. In recent decades, the aerospace industry has witnessed a revolutionary transformation in the production of composite structures through automated manufacturing techniques such as AFP [26]. These methods offer various advantages, including enhanced precision in fibre placement, automated debulking, and the elimination of post-processing steps like oven or autoclave curing [27]. Furthermore, they contribute to reductions in material and labor costs [28]. Consequently, major manufacturers like Boeing, Airbus and NASA have adopted these techniques extensively to manufacture highly precise components like wing skins, nose cones, and fuselages [29–32]. Additionally, ongoing studies are exploring the utilization of these methods into other sectors and industries like marine, automotive and wind energy for making composite propellers, wheels and turbine blades [29–31, 33–37].

1.3 Composite Materials: Structures and Types

A composite material is formed by combining two or more different materials, each of which possesses distinct physical or chemical properties. When these materials are combined, they create a new material with unique characteristics. Composites are widely used in many applications across multiple industries, including aerospace, marine, aviation, transportation, sports, and civil engineering [38]. The categorization of composites based on the types of reinforcement and matrix materials is depicted in Fig. 3.

Among them, laminated and sandwich panels are increasingly utilized for structural purposes [39, 40]. Laminated composites are created by bonding multiple layers (referred to as ply or lamina) together. Each layer consists of strong, continuous fibres that provide reinforcement, surrounded by a comparatively weaker matrix material. The use of carbon fibre reinforced polymers (CFRP) and glass fibre reinforced plastic (GFRP) composites in structural components has greatly expanded in various fields including aircraft, sports vehicles, wind turbines, and infrastructure projects [26]. For instance, the new Boeing 787 Dreamliner aircraft incorporates composite materials accounting for ~52% of its weight [41], and the new Airbus A380 utilizes composites that makeup ~25% of its weight [42]. The exceptional properties of laminated composites, such as a high strength-to-weight ratio, resistance to creep, high tensile strength at high temperatures, and toughness, have sparked increasing interest across different industries [38, 43]. Another key driver for the industry's adoption of composite materials is the advantage of reduced weight, leading to substantial cost savings, energy efficiency improvements up to 18%, and lower CO_2 emissions [44]. Figure 4 shows the application of FRPC in different industries.

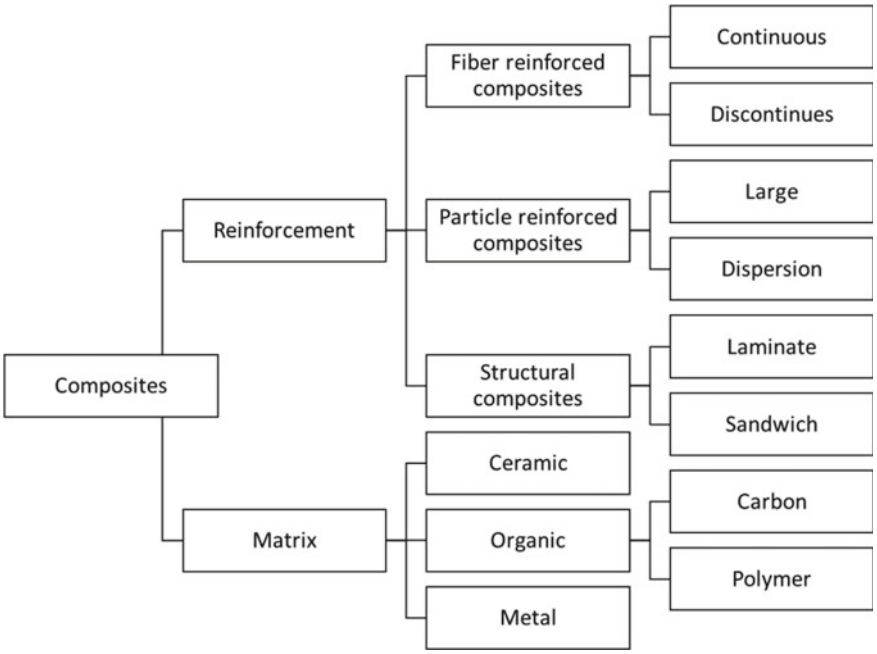

Fig. 3 Classification of composites based on reinforcement and matrix materials

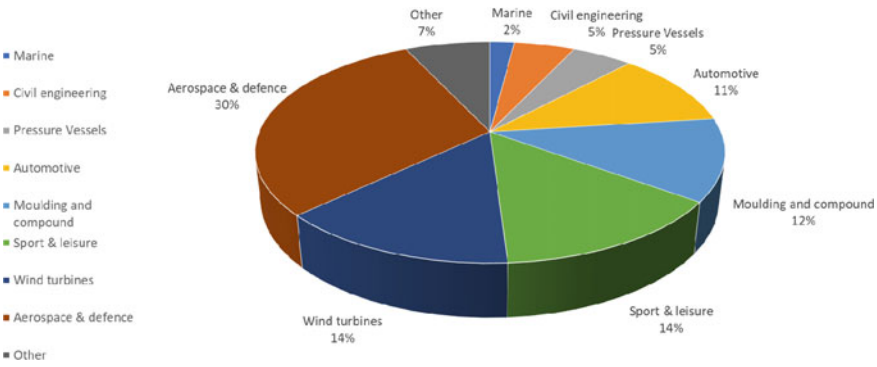

Fig. 4 Application of fibre reinforced polymer composites in Europe for different industry sectors [45]

1.3.1 Composite Materials for AFP

Prepreg tapes are commonly utilized in AFP. They consist of carbon or glass fibres impregnated with a thermosetting or thermoplastic resin matrix. They are available

in rolls of different widths and are characterized by factors such as resin content, self-adhesive strength, drapeability, shelf life, and gel time. In prepregs, the reinforcing fibres are pre-impregnated with a partially cured resin to a specific level. This allows the prepreg tapes to be directly placed into a mould without the need for additional resin. However, heat and pressure must be applied during the manufacturing process to ensure a strong bond. In the case of thermoplastic composites, when the heated surfaces of the tape and substrate come into contact under pressure, the polymer chains diffuse between the matrix layers of each surface through thermal vibrations, forming a bond. The bonded area is then cooled under pressure at room temperature [28]. Thermoset prepregs, on the other hand, require controlled heat during the curing process. This heat allows the resin to flow within the laminate and polymerize, ultimately reaching the cured state [46].

Prepregs offer several advantages over non-impregnated tapes and fibres, including enhanced maximum strength properties, uniformity, consistent quality, and reduced material wastage. However, they are relatively expensive, require heat for processing, and require special storage conditions [47, 48].

As mentioned earlier, prepregs are categorized into two main types based on their polymer matrix: thermosets and thermoplastics. Thermoset matrices are the most used and are cost-effective materials that exhibit resistance to solvents. They undergo irreversible curing through the application of heat or suitable irradiation [49]. Epoxy resin is the most prevalent thermoset materials, offering superior performance at a relatively low cost. On the other hand, thermoplastic matrices can be softened by heating them to their processing temperatures. The process is reversible since no cross linking occurs. The choice of polymer matrix depends on the specific application requirements [44, 50, 51]. An evaluation of these two matrix types, considering their processing benefits, is discussed in [52].

2 Recent Studies

The viability of three novel approaches, including ISF, FW, and LAR, for retrofitting stone columns has been examined by Cascardi et al. [20]. Through axial compressive tests, it was demonstrated that the proposed techniques did not compromise the effectiveness of confinement. The examination of the substrates after the tests confirmed the reversibility of the proposed solutions, as evidenced by the absence of detachment of the stone surface. The investigated retrofitting techniques demonstrated their potential to serve as a valuable and efficient methods for increasing the seismic protection of columns in heritage buildings.

Mohammed et al. [8] conducted a comprehensive review of the current practices and potential applications of prefabricated composite jackets for structural repair. According to their findings, prefabricated FRP composite repair systems are considered preferable to wet lay-up methods due to their ease of installation, improved safety measures, higher quality, minimized on-site workforce needs and minimized resource wastage. However, the design of effective joints, that facilitate easy, quick,

and safe installation, plays a crucial role in ensuring structural continuity when using prefabricated FRP composite jackets. The effectiveness of prefabricated FRP composite jackets depends on factors such as fibre thickness, orientation, the properties of the infill grout, and the extent and shape of existing structural damage. Thus, a thorough understanding of these design parameters is essential for achieving an optimal and safe design for prefabricated FRP jacket repair systems. Additionally, the existing models for predicting the strength and behaviour of structures strengthened with FRP composite jackets often overlook the level of damage present in the original structures. Hence, it is necessary to develop numerical and/or analytical models that systematically account for the influence of key parameters on the overall response of repaired structures. This will result in a more reliable and secure repair system.

Zeng et al. [53] have investigated the behaviour of fibre reinforced polymer (FRP) confined elliptical concrete-filled steel tube (ECFST) columns and the effects of various factors including the FRP jacket thickness and the cross-sectional aspect ratio. The authors aimed to (a) examine the efficiency and benefits of FRP confinement to ECFST columns under axial compression, (b) understand the behaviour of confined concrete in FRP-confined ECFSTs, and (c) examine the capability and accuracy of existing theoretical models for concrete in FRP-confined ECFSTs. Considering the high vulnerability of high-strength steel (HSS) to buckling, Q690 steel tubes were utilized in this study. According to their findings, an FRP jacket significantly improves the elastic stiffness, yield axial load, and ultimate axial load of ECFST columns. It was also shown that, the axial load-strain behaviour of ECFST columns can be divided into two segments. An ascending linear segment, which is connected to a secondary section can exhibit either an upward trend or a downward trend.. The confinement mechanism of concrete in FRP-confined ECFST columns resembles that of FRP-confined concrete, whose axial stress–strain curve typically exhibits a bilinear behaviour. Both the ultimate axial stress and ultimate axial strain increase with increasing FRP jacket thickness at a given cross-sectional aspect ratio. However, for a given FRP jacket thickness, the confinement efficiency decreases as the cross-sectional aspect ratio increases, leading to lower ultimate axial stress and a shallower slope of the second ascending portion. FRP-confined ECFST specimens with a cross-sectional aspect ratio of 2.0 exhibit poor FRP confinement efficiency. An increase in cross-sectional aspect ratio results in a decrease in ultimate axial stress and ultimate axial strain. The enhancement index for elastic stiffness increases with the cross-sectional aspect ratio for specimens with a given FRP thickness. This indicates that the FRP jacket is more effective in improving the elastic stiffness of ECFST columns compared to circular concrete-filled steel tube (CCFST) columns[53].

In the following section, the effectiveness of a new automated technique to retrofit short columns and beams is discussed. For this purpose, the behaviour of short steel columns and beams overwrapped with thermoplastic carbon fibres using AFP is presented.

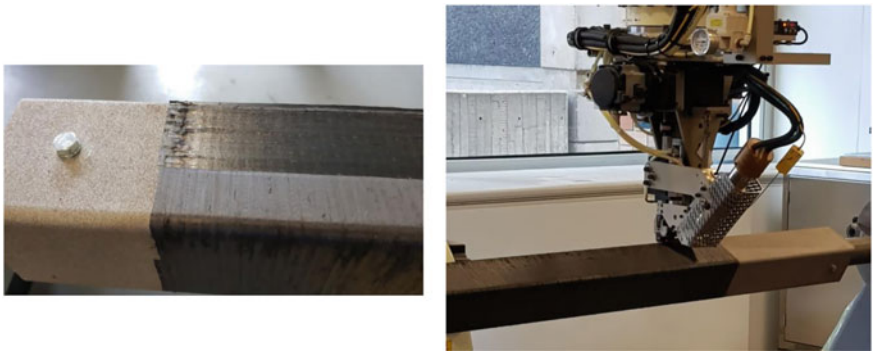

Fig. 5 Over wrapping steel profiles with thermoplastic CFRP using AFP. *Photo courtesy* Automated Composites Laboratory, UNSW Sydney

3 Experimental Program

3.1 Sample Preparation

The Automated Dynamics-built AFP machine at UNSW Sydney was utilized for reinforcing the SHS specimens, as shown in Fig. 5. This AFP machine is a seven-axis robot platform, including a coordinated spindle. The thermoplastic placement head comprises of a consolidation system, prepreg tape dispensing system, hot gas torch (HGT) as a heat source (Fig. 2), and a computer controller [25]. Carbon-PEEK prepreg tapes (AS4/APC2, supplied by Solvay) were used to reinforce the steel profiles. The prepreg tapes were 0.15 mm thick and 6.35 mm wide. The key material properties of the prepreg tape of density, modulus of elasticity, shear modulus, Poisson's ratio and fibre volume fraction were 1570 kg/m^3, 138 GPa, 5 GPa, 0.28 and 0.6, respectively.

The AFP deposition rate, HGT temperature and consolidation force were selected based on the authors' earlier investigations [54–59] and set as 76 mm/s, 900 °C and 200 N, respectively. The layup sequences were chosen to ensure a strong and durable bond between the prepreg and SHS for all reinforced profiles and are summarized in Tables 1 and 2. The surface of the steel profiles was sandblasted using Class 2.0 blast with a GL40 steel grit size.

3.2 Column Specimens

Fourteen column specimens made up of SHS were tested under axial compression for the determination of the ultimate load. The steel profiles were 3.5 mm thick with cross sectional outer dimensions of 89 mm × 89 mm according to Standards Australia Online [60]. As shown in Table 1, the length of each column was 267 mm, three times

Table 1 Details of the column specimens

Specimen		Direction (T/L)	Lay-up	Overwrapped with CF-PEEK
C	a	–	–	No
	b	–	–	No
1	a	T	[90, 90]	Yes
	b	T	[90, 90]	Yes
	c	T	[90, 90]	Yes
	d	T	[90, 90]	Yes
2	a	L	[0, 0]	Yes
	b	L	[0, 0]	Yes
	c	L	[0, 0]	Yes
	d	L	[0, 0]	Yes
	e	L	[0, 0]	Yes
	f	L	[0, 0]	Yes
	g	L	[0, 0]	Yes
	h	L	[0, 0]	Yes

Note T = Transverse, L = Longitudinal

Table 2 Details of the tested beam specimens

Specimen		Direction (H/V)	Lay-up	Overwrapped with CF-PEEK
B	a	–	–	No
	b	–	–	No
3	a	H	[0, 0]	Yes
	b	H	[0, 0]	Yes
4	a	H	[0, 0]	Yes
	b	H	[0, 0]	Yes
5	a	V	[90, 90]	Yes
	b	V	[90, 90]	Yes
6	a	V, 45°	[90, 90, 45]	Yes
	b	V, 45°	[90, 90, 45]	Yes
7	a	V	[90, 90]	Yes
	b	V	[90, 90]	Yes
8	a	HV	[90, 0]	Yes
	b	HV	[90, 0]	Yes
9	a	HV	[90, 0]	Yes
	b	HV	[90, 0]	Yes

Note H = Horizontal; and V = Vertical

that of the breadth of the specimen. The measured lengths of the columns ranged from 267 to 269 mm. Two control column specimens (C-a and C-b) were tested under axial compression (Fig. 6). The control columns did not have thermoplastic carbon fibre reinforced polymer (CFRP). Twenty-one specimens were externally reinforced with thermoplastic CFRP plies AFP machine at UNSW Sydney. Four specimens (1-a, 1-b, 1-c and 1-d) had two layers of thermoplastic CFRP laid transversally (perpendicular to axial loading) as shown in Fig. 7. Additionally, eight columns (2-a, 2-b, 2-c, 2-d, 2-e, 2-f, 2-g and 2-h) had two layers of thermoplastic CFRP plies laid longitudinally (parallel to axial loading), see Fig. 8. Two Stainless Steel Hose Clamps were installed on specimens (1-c, 1-d, 2-c, 2-d, 2-e, 2-f, 2-g and 2-h) to find out if the ultimate loads of the CFRP strengthened columns with steel hose clamps increase in comparison to the CFRP strengthened columns with no steel hose clamps. Steel hose clamps were trailed as the CFRP plies that were laid longitudinally on column specimens separated from the steel under axial compression loading. The location of the stainless-steel hose clamps is shown in Fig. 9.

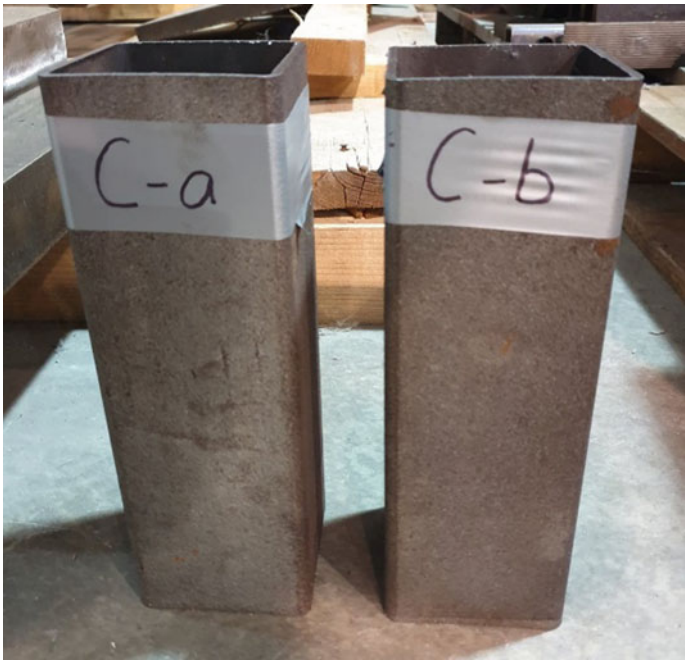

Fig. 6 Control column specimens

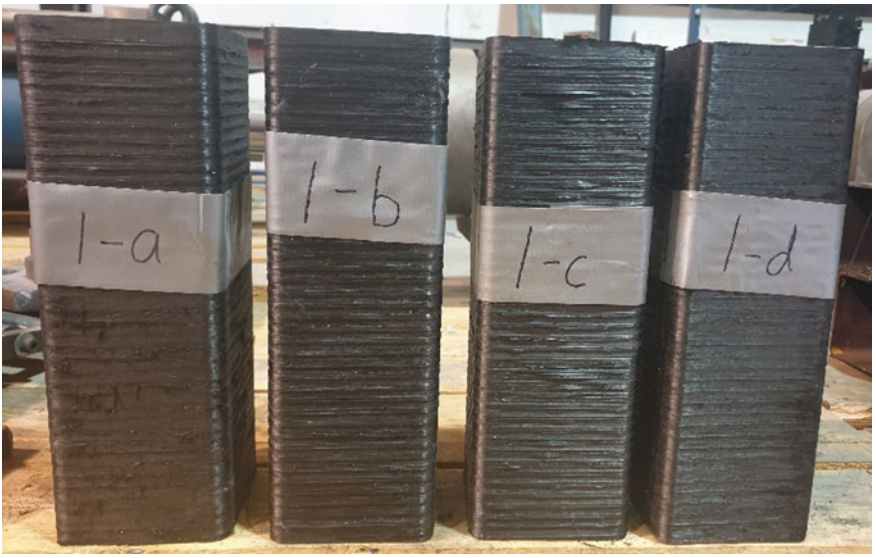

Fig. 7 Transverse reinforced column specimens

Fig. 8 Longitudinal reinforced column specimens

3.3 Beam Specimens

Two control beams and fourteen thermoplastic CFRP overwrapped beams shown in Table 2 were tested for their bending capacity. The steel beam specimens were in the

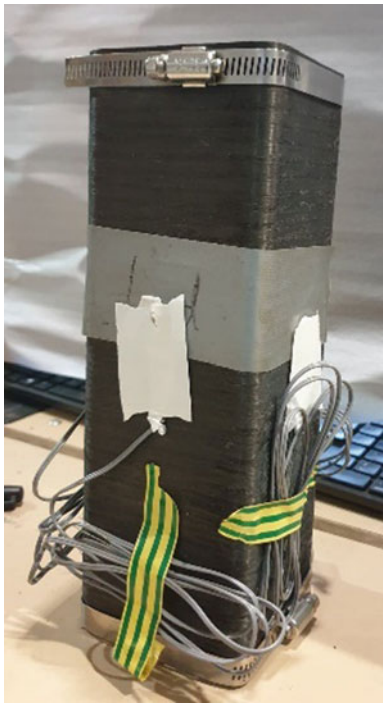

Fig. 9 Locations of stainless-steel hose clamps

form SHS with thickness of 3.5 mm and cross-sectional outer dimensions of 89 mm × 89 mm. The length of each beam was approximately 750 mm.

As shown in Fig. 10, the control beams (B-a and B-b) did not have thermoplastic CFRP wrap. Beam specimens (3-a, 3-b, 4-a and 4-b) had two layers of CFRP plies laid horizontally (parallel to length), as in Fig. 11. Specimens (5-a, 5-b, 7-a and 7-b) had two layers of CFRP laid vertically (perpendicular to length), as shown in Fig. 12. Beam specimens (6-a and 6-b) shown in Fig. 13 were made with three layers of CFRP placed vertically and at angle of 45°. Beam specimens (8-a, 8-b, 9-a and 9-b) shown in Fig. 14 had two layers of CFRP laid horizontally and vertically.

Fig. 10 Control beam specimens

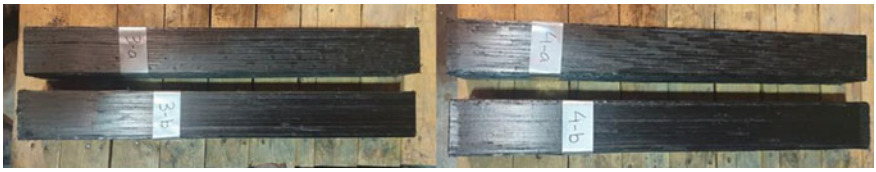

Fig. 11 Longitudinal reinforced beam specimens

Fig. 12 Transverse reinforced beam specimens

Fig. 13 Reinforced beam specimens with additional layer of 45°

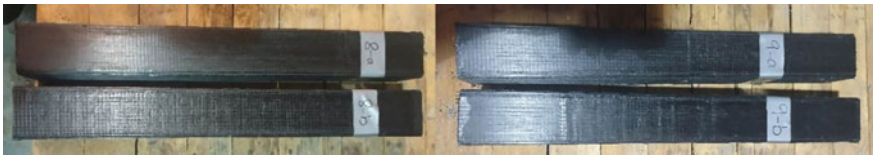

Fig. 14 Transverse and longitudinal beam reinforced specimens

3.4 Instrumentation and Testing of Column Specimens

Axial deformations were measured using a linear potentiometer (LP1516). This is detailed in Fig. 15. Two control columns and twelve CFRP columns were tested under axial compressive loading using a compression test machine shown in Fig. 16. The column specimens had a fixed support at the base of the column with the load being applied to the top of the column via a flat plate (see Fig. 16). For determining

the peak load, the test specimens were subjected to a continuous axial compressive load applied at a rate of 0.016 mm/s. The test continued at the same rate after the peak load was obtained and then was stopped when the load reduced to a value of 300 kN for control columns and 150 kN for CFRP columns.

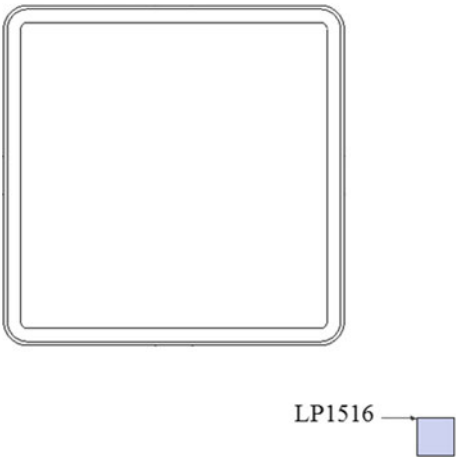

Fig. 15 Plan view of instrumentation locations

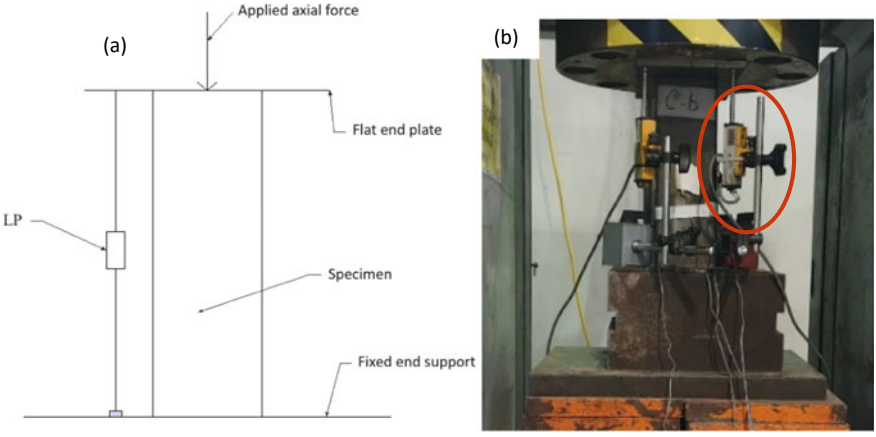

Fig. 16 Test setup: **a** Schematic diagram and **b** test setup in compression-testing machine showing LP1516

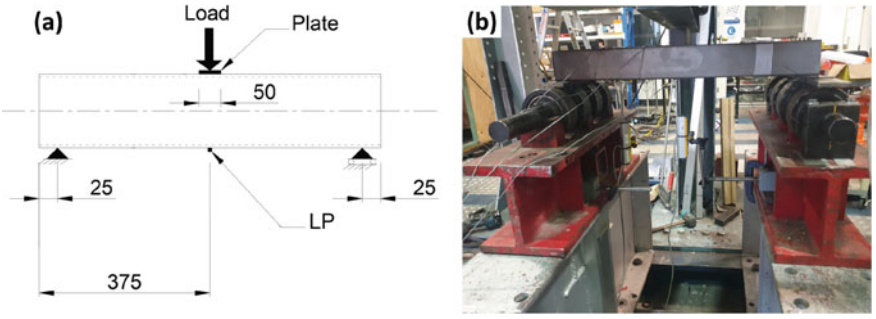

Fig. 17 Test setup: **a** schematic diagram and **b** test rig (all dimensions are in mm)

3.5 Instrumentation and Testing of Beam Specimens

A liner potentiometer (LP) was used at the bottom face of the beams to measure deflections, see Fig. 17a. The bending capacity of the control beams and 4 CFRP strengthened beams were investigated using the test setup shown in Fig. 17a. Loads were applied at the midspan of the beams using a hydraulic jack, as shown in Fig. 17b. The control beam behaviour was compared to the different methods of strengthening using CFRP. The beam specimens were pin connected at both ends of each beam. The pinned supports were located 25 mm away from the end edges of the beam. The load was applied to these test specimens at a rate of 0.016 mm/s. The test continued at the same rate after obtaining the peak load until the load dropped to a value of 49 kN or the specimens failed.

4 Performance Prediction of Reinforced Steel Profiles

4.1 Strength of Steel Beams Reinforced with Thermoplastic Carbon Fibre Reinforced Polymer

4.1.1 Behaviour of Beams

The ultimate loads for the SHS control beams and CFRP beams are shown in Table 3. There is a good agreement between the predicted ultimate compressive loads (Standards Australia Online [61] and OneSteel Market Mills [62]) and experimental ultimate compressive loads. The predicted value of the ultimate load for the control beams was 93.9 kN. The values of the experimental ultimate load of specimens B-a and B-b were 87.2 and 77.8 kN, respectively.

The ultimate load of B-b was lower than B-a. This may be because the weld line of B-b was on the bottom surface (Fig. 18) whereas the weld line of B-a was on the

Table 3 Experimental values of ultimate loads

Specimen		Direction (H/V)	Lay-up	Ultimate load (kN)
B	a	–	–	87.21
	b	–	–	77.82
3	a	H	[0, 0]	81.85
	b	H	[0, 0]	82.73
4	a	H	[0, 0]	86.24
	b	H	[0, 0]	85.99
5	a	V	[90, 90]	83.30
	b	V	[90, 90]	88.81
6	a	V, 45°	[90, 90, 45]	82.98
	b	V, 45°	[90, 90, 45]	87.26
7	a	V	[90, 90]	73.59
	b	V	[90, 90]	72.40
8	a	HV	[90, 0]	74.15
	b	HV	[90, 0]	76.21
9	a	HV	[90, 0]	84.33
	b	HV	[90, 0]	83.57

top surface. This shows SHS beams may carry higher load when the weld line is on the top surface.

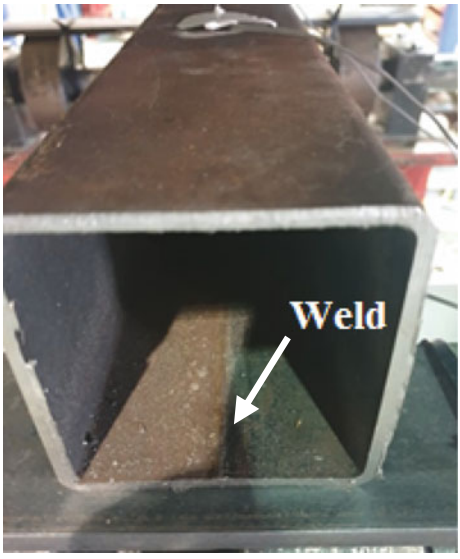

Fig. 18 Weld line of specimen B-b

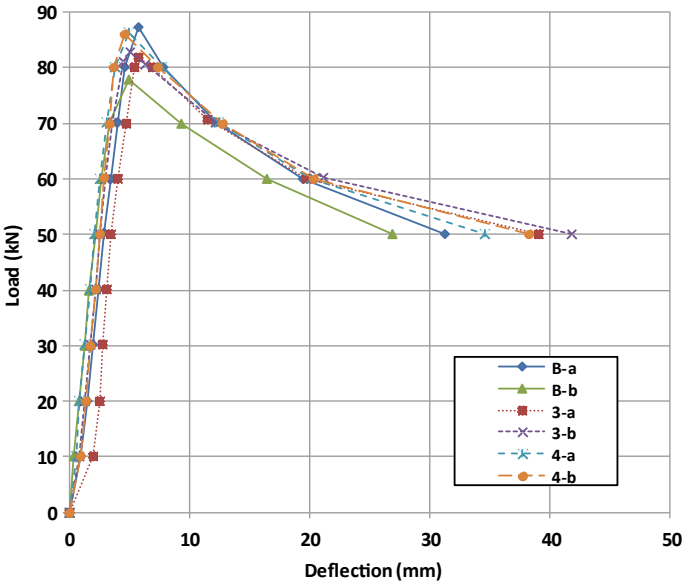

Fig. 19 Load–deflection curves for the control beams and longitudinally reinforced CFRP beams

The load–deflection curves of the control beams and specimens 3-a, 3-b, 4-a and 4-b with longitudinal CFRP reinforcement are shown in Fig. 19. The values of the experimental ultimate load of specimens 3-a, 3-b, 4-a and 4-b beams are 81.9, 82.7, 86.2 and 86.0 kN, respectively. These values are higher than the ultimate load of specimen B-b of 77.8 kN. Specimens 3 and 4 were compared with control beam B-b as the weld lines of beams 3, 4 and B-b were not located on the top surface.

The load–deflection curves of specimens 5-a, 5-b, 7-a and 7-b with transverse CFRP reinforcement are shown in Fig. 20. The values of the experimental ultimate load of specimens 5-a, 5-b, 7-a and 7-b beams were 83.3, 88.8, 73.6 and 72.4 kN, respectively. The ultimate load of CFRP beam 5-a (83.3 kN) was greater than the ultimate load of control beam B-b (77.8 kN). CFRP beam 5-a was compared with control beam B-b as the weld lines of these beams was not located on the top surface. The ultimate load of CFRP beam 5-b (88.8 kN) was greater than the ultimate load of control beam B-a (87.2 kN). The weld lines of specimens 5-b and B-a were located on the top surface. The ultimate loads of CFRP beams 7-a and 7-b were 73.6 and 72.4 kN, respectively. These values were lower than the ultimate loads of control beams.

The load–deflection curves of specimens 6-a and 6-b with CFRP reinforcement at 45° are shown in Fig. 21. The values of the experimental ultimate loads for specimens 6-a and 6-b beams were 83.0 and 87.3 kN, respectively. These values were greater than the ultimate load of control beam C-b (77.8 kN) and were lower than the ultimate load of control beam C-a (87.2 kN).

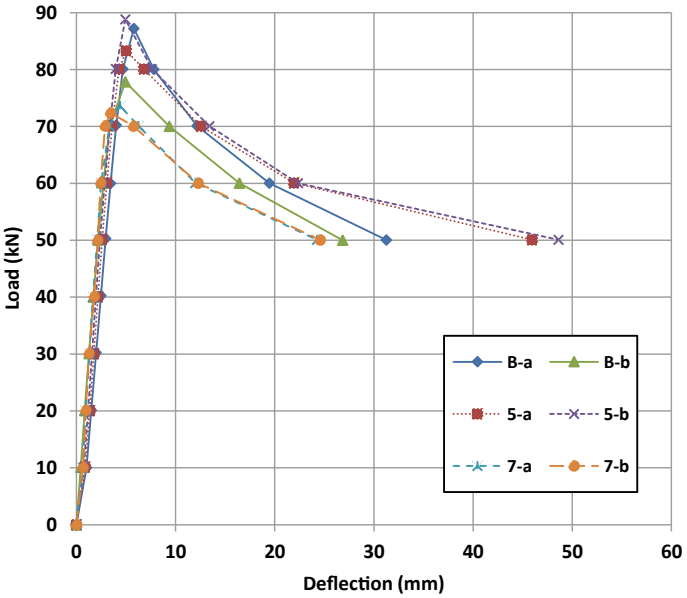

Fig. 20 Load–deflection curves for the control beams and transversally reinforced CFRP beams

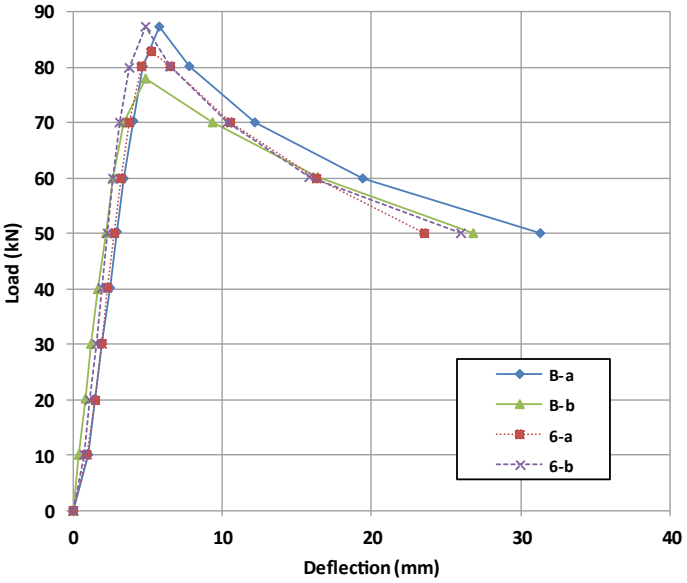

Fig. 21 Load–deflection curves for the control beams and beams with CFRP reinforcement at 45°

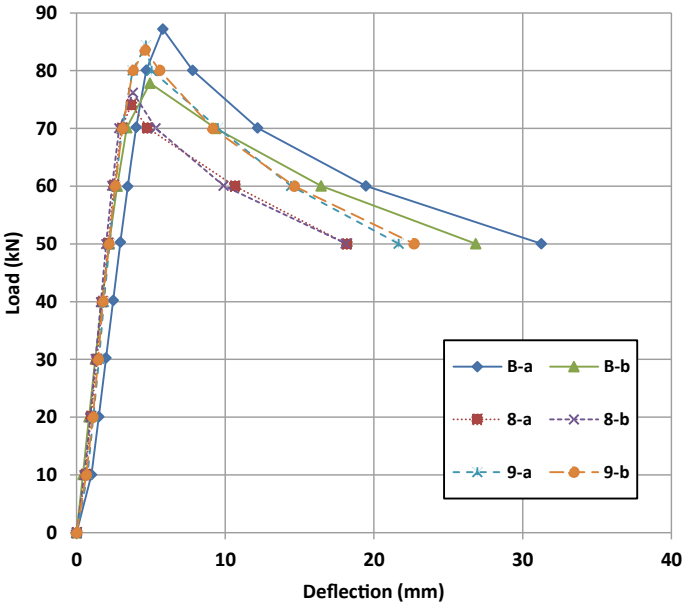

Fig. 22 Load–deflection curves of control beams and beams with CFRP laid longitudinally and transversally

The load–deflection curves for specimens 8-a, 8-b, 9-a and 9-b with longitudinal and transverse reinforcement are shown in Fig. 22. The values of the experimental ultimate load of specimens 8-a, 8-b, 9-a and 9-b beams were 74.2, 76.2, 84.3 and 83.6 kN, respectively. The ultimate loads for the strengthened beams 8-a, 8-b, 9-a and 9-b were similar to that of the control beams.

4.1.2 Failure Modes

For the SHS beams with and without thermoplastic CFRP overwrap, local deformations were observed at the location of the load application. As shown in Fig. 23, there was inward deformation (concave) on the upper surface of each beam. Outward deformations (convex) were observed on the two side walls of the beams.

For beam specimens 3-a, 3-b, 4-a and 4-b with CFRP laid longitudinally, the CFRP composites separated from steel SHS, see Fig. 23b for a typical failure mode. For beam specimens 5-a, 5-b, 7-a and 7-b whose CFRP was laid transversally, the thermoplastic CFRP layers snapped as the load was applied to the specimens, see Fig. 23c for a typical failure mode. Figure 23d shows a typical failure mode for a beam specimen whose CFRP was laid at an angle of 45°. The 45° CFRP layers de-bonded from the thermoplastic transverse CFRP at the location of the load (top and sides locations). For beam specimens 8-a, 8-b, 9-a and 9-b whose CFRP was

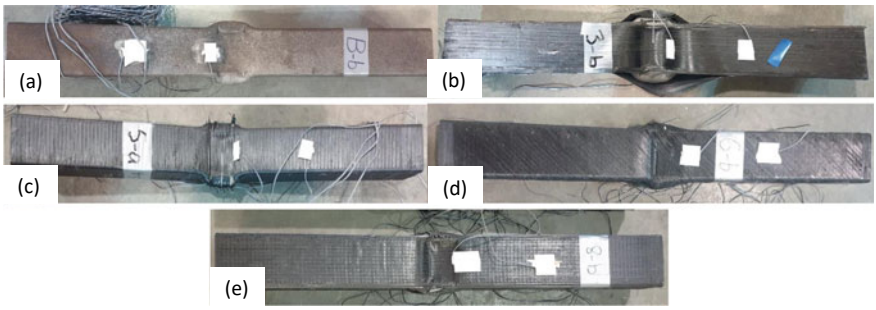

Fig. 23 Typical failure modes of the SHS beams: **a** B-b; **b** 3-b; **c** 5-a; **d** 6-b; and **e** 8-b

laid longitudinally and transversally, de-bonding of the thermoplastic CFRP from the steel tube were observed at the corners, as shown in Fig. 23e.

4.2 Axial Strength of Steel Short Columns Reinforced with Thermoplastic Carbon Fibre Reinforced Polymer (CFRP)

4.2.1 Behaviour of Columns

The ultimate loads and the deflections at ultimate load for the two SHS control columns and twelve CFRP columns are shown in Table 4. For control columns, a good agreement was observed between the predicted and experimental ultimate compressive loads. The experimental ultimate load of C-a and C-b were 527.9 and 524.1 kN, respectively. According to Standards Australia Online [61] and, OneSteel Market Mills [62], the predicted value of the ultimate load for the control columns was 517.5 kN (Table 4). As shown in Table 4, Figs. 24 and 25, the ultimate loads for the thermoplastic CFRP columns did not exceed the ultimate loads for the control columns.

4.2.2 Failure Modes

The failure modes for the steel SHS control columns were local buckling failure, as shown in Fig. 26a. Both inward and outward buckling were observed in the control columns. Bottom end buckling occurred on specimen C-a and top end buckling can be observed on specimen C-b. Inward and outward buckling are also observed in the transverse CFRP columns. As shown in Fig. 26b, bottom end buckling occurred on specimen 1-a, 1-b and 1-c whereas top end buckling can be observed on specimen 1-d. Also, the CFRP layers for the transversally reinforced CFRP columns with

Table 4 Ultimate loads and deflections for SHS columns

Specimen		Direction (T/L)	Steel Hose Clamps installed on column	Ultimate load (kN)
C	a	–	No	527.94
	b	–	No	524.08
1	a	T	No	478.10
	b	T	No	507.88
	c	T	Yes	493.00
	d	T	Yes	513.63
2	a	L	No	484.53
	b	L	No	499.46
	c	L	Yes	448.13
	d	L	Yes	404.03
	e	L	Yes	494.51
	f	L	Yes	491.50
	g	L	Yes	498.04
	h	L	Yes	504.20

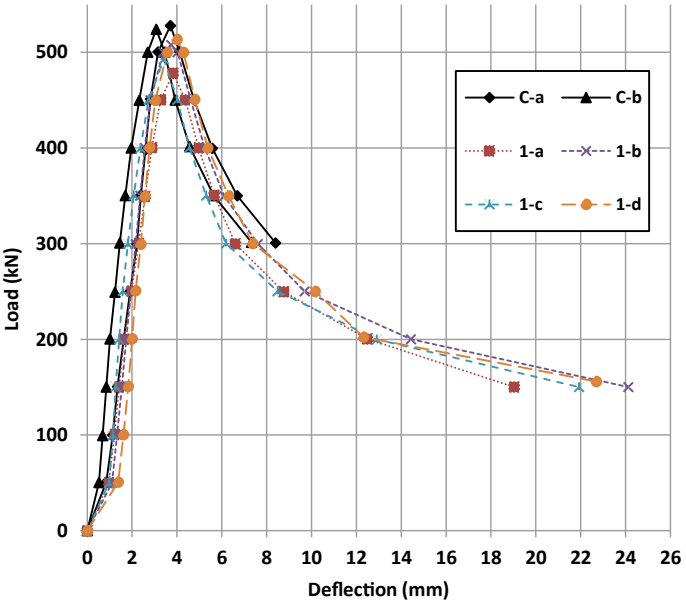

Fig. 24 Load–deflection curves for control columns and transversally reinforced CFRP columns

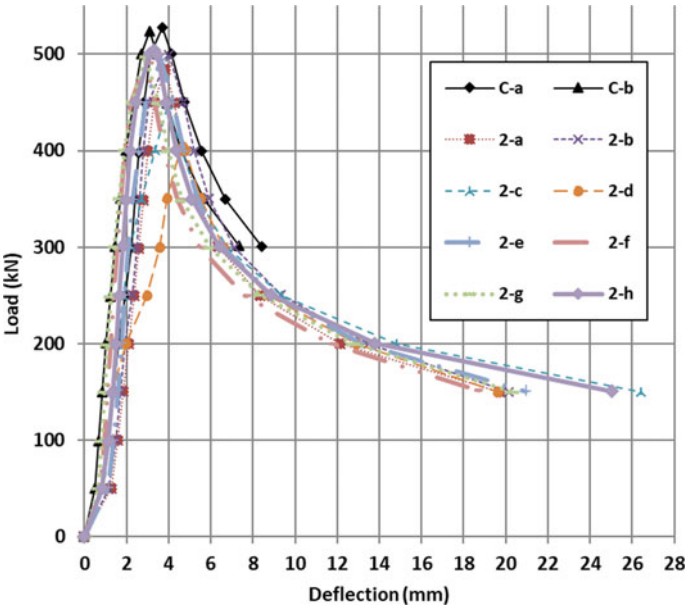

Fig. 25 Load–deflection curves for control columns and longitudinally reinforced CFRP columns

and without steel hose clamps snapped as the compression load was applied on the specimens. Inward and outward buckling were also observed in the longitudinal CFRP columns. Bottom end buckling occurred on specimen 2-b, 2-e and 2-f. Top end buckling was observed on specimens 2-a, 2-c, 2-d, 2-g and 2-h, see Fig. 26c. As shown in Fig. 26c, de-bonding of the CFRP plies can be observed in specimens without steel hose clamps (specimens 2-a and 2-b). For specimens with steel hose clamps, the CFRP steel did not completely separate when the specimens were subjected to compression loads. Furthermore, as shown in Fig. 26c, the steel hose clamps located on the top edge of specimens 2-d and 2-g snapped under the compression load. Tearing of CFRP plies on the corners of specimen 2-g and 2-h was also observed.

5 Discussion and Conclusion

Cold-formed SHS beams and columns are widely used in engineering structures such as bridges, cranes, and towers. In engineering structures, these sections are often subjected to cyclic loading from imposed loads such as vehicles and wind loads. When loads are applied to a structure, cracks may initiate and propagate, and subsequent fatigue failure may occur. Improving the mechanical behaviour of such structures can be achieved with CFRP reinforcement in the form of a jacket. The utilization of FRPC jackets provides a range of significant advantages including

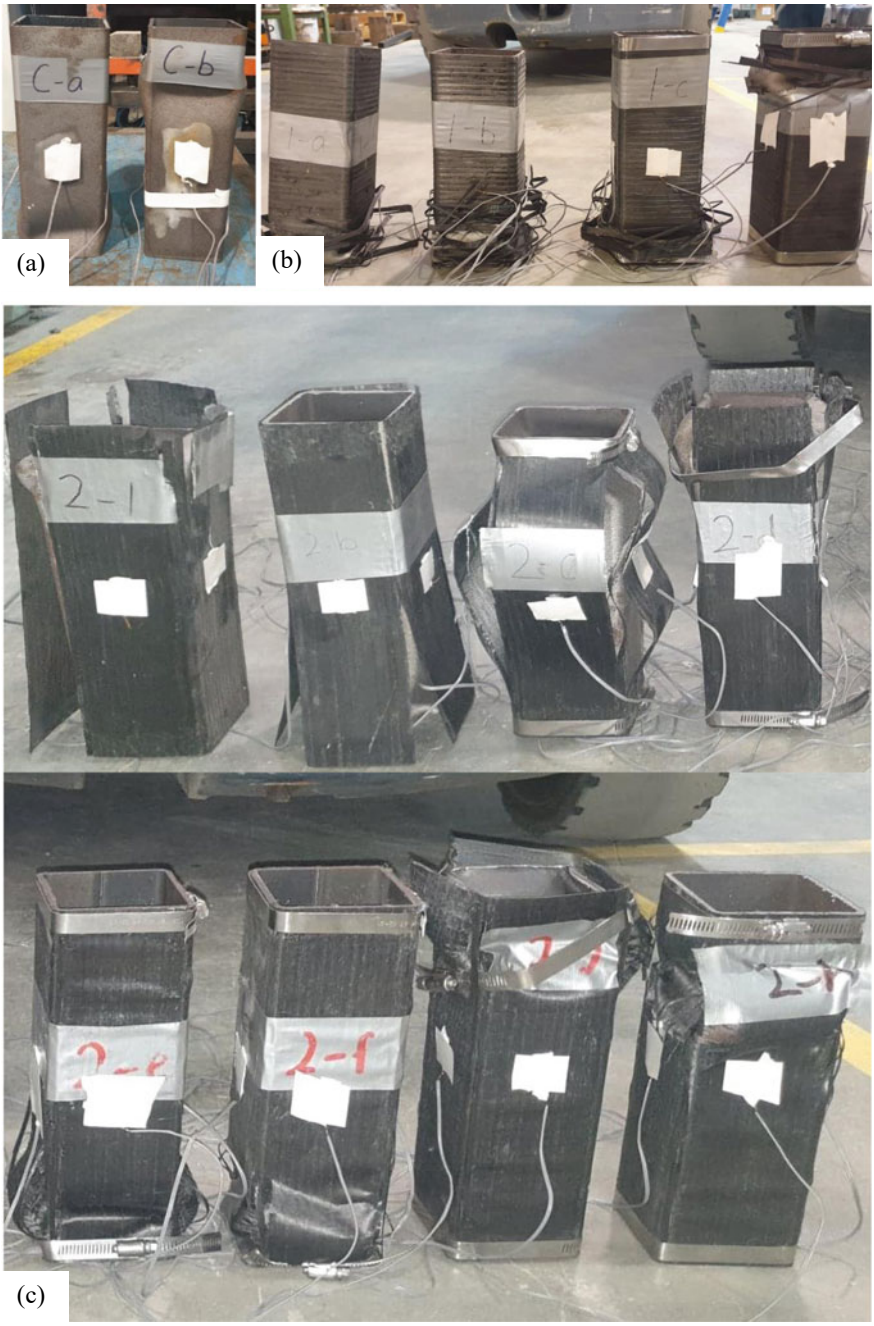

Fig. 26 Failure mode of: **a** control columns, **b** transverse CFRP columns with and without steel hose clamps, and **c** longitudinal CFRP columns with and without steel hose clamps

superior resistance to corrosion, durability and long-life compared to the limitations of conventional repair systems such as concrete and steel jackets. This experimental investigation presented in this chapter focused on reinforcing thin-walled SHS columns and beams with thermoplastic CFRP using hot gas torch assisted automated fibre placement. Fourteen SHS column specimens were tested under axial compression for determination of their ultimate loads. Two control beams and fourteen thermoplastic CFRP overwrapped beams were also tested for the determination of their bending capacity. The results obtained from this investigation were compared with the baseline samples without CFRP and are summarized below,

- For the control beams, there was a good agreement between the predicted ultimate compressive loads and experimental ultimate compressive loads.
- The experimental ultimate load of thermoplastic CFRP beams did not show significant improvement using the current AFP strengthening method due to the failure modes. For beam specimens whose CFRP was laid longitudinally, the thermoplastic CFRP plies separated from the steel. For beam specimens whose CFRP was laid transversally, some thermoplastic CFRP layers snapped as the load was applied on the specimens. For beam specimens whose CFRP was laid at an angle of 45°, the CFRP layers de-bonded from the thermoplastic transverse CFRP at the location of the load. For beam specimens whose CFRP was laid longitudinally and transversally, de-bonding of the thermoplastic CFRP from the steel tube was observed at the corners. For the SHS beams with and without thermoplastic CFRP, inward deformation was observed on the upper surface of each beam and outward deformation was observed on the two side walls of the beams.
- For the control columns, a good agreement was observed between the predicted and experimental ultimate compressive loads. The ultimate loads of the CFRP columns were lower than the ultimate loads for the control columns. De-bonding, tearing and snapping of the CFRP plies are observed in specimens with thermoplastic CFRP.

This investigation is still ongoing, as further research is being conducted to explore the effect of factors such as the number of overwrapped plies, ply orientation, and AFP processing conditions on the strength of reinforced SHS profiles. These continued efforts aim to enhance our understanding of FRP composite jacketing techniques and optimize their application in structural repairs.

Acknowledgements This project was funded by Western Sydney University (WSU) and University of New South Wales (UNSW). The authors would like to acknowledge the support received through following funding schemes of Australian Government:

ARC LIEF: An Australasian facility for the automated fabrication of high-performance bespoke components (LE140100082).

ARC ITTC: ARC Training Centre for Automated Manufacture of Advanced Composites (IC160100040).

References

1. Kumar Nigam P, Akhtar S (2021) Retrofitting practices in various categories of RCC structures—a comprehensive review. Mater Today: Proc 45:7123–7131
2. 10 Best Retrofitting Techniques for RCC Buildings [Internet]. Civil String Get the Knowledge (2021). Available from: https://civilstring.com/retrofitting-techniques-for-rcc-buildings/
3. Waghmare SPB (2011) Materials and jacketing technique for retrofitting of structures. Int J Adv Eng Res Stud 1(1):15–19
4. FRP Jacketing versus Steel Jacketing—structural strengthening. In: Horse (ed) Solutions (2023)
5. Di Trapani F, Malavisi M, Marano G, Greco R, Ferrotto M (2020) Optimal design algorithm for seismic retrofitting of RC columns with steel jacketing technique. Procedia Manuf 44:639–646
6. Samy K, Fawzy A, Fouda MA (2023) Strengthening of historic reinforced concrete columns using concrete and FRP jacketing techniques. Asian J Civil Eng 24(3):885–896
7. Ozbakkaloglu T (2013) Compressive behavior of concrete-filled FRP tube columns: assessment of critical column parameters. Eng Struct 51:188–199
8. Mohammed AA, Manalo AC, Ferdous W et al (2020) State-of-the-art of prefabricated FRP composite jackets for structural repair. Eng Sci Technol Int J 23(5):1244–1258
9. Li G, Kidane S, Pang S-S, Helms JE, Stubblefield MA (2003) Investigation into FRP repaired RC columns. Compos Struct 62(1):83–89
10. Saafi M, Asa E (eds) (2010) Extending the service life of electric distribution and transmission wooden poles using a wet layup FRP composite strengthening system. J Perform Constructed Facil
11. Teng JG, Yu T, Fernando D (2012) Strengthening of steel structures with fiber-reinforced polymer composites. J Constr Steel Res 78:131–143
12. Roads V (ed) (2018) Code of practice: FRP for strengthening of bridge structures
13. Kim H, Lee KH, Lee YH, Lee J (2012) Axial behavior of concrete-filled carbon fiber-reinforced polymer composite columns. Struct Design Tall Spec Build 21(3):178–193
14. Vincent T, Ozbakkaloglu T (2013) Influence of fiber orientation and specimen end condition on axial compressive behavior of FRP-confined concrete. Constr Build Mater 47:814–826
15. Teng J, Chen J-F, Smith ST, Lam L (2002) FRP: strengthened RC structures
16. Wu R-Y, Pantelides CP (2017) Rapid repair and replacement of earthquake-damaged concrete columns using plastic hinge relocation. Compos Struct 180:467–483
17. Lam L, Teng JG (2003) Design-oriented stress–strain model for FRP-confined concrete. Constr Build Mater 17(6):471–489
18. Mazumdar SK (2002) Composites manufacturing: materials, product, and process engineering. CRC Press LLC, United States of America
19. Performance Proven Worldwide. Wet Lay-Up Process United States of America: Performance Proven Worldwide; cited 2015. Available from: http://www.pactinc.com/capabilities/wet-lay-uphand-lay-up-method/
20. Cascardi A, Dell'Anna R, Micelli F, Lionetto F, Aiello MA, Maffezzoli A (2019) Reversible techniques for FRP-confinement of masonry columns. Constr Build Mater 225:415–428
21. Gutowski T (1997) Advanced composites manufacturing. Wiley, New York, p 600
22. August Z, Ostrander G, Hauber D (eds) (2015) Additive manufacturing with high performance thermoplastic composites. In: The second international symposium on automated composites manufacturing. Montreal, Canada
23. Werner D (ed) (2015) Multi-material-head novel laser-assisted tape, prepreg and dry-fiber placement system. In: The second international symposium on automated composites manufacturing. Montreal, Canada
24. Stokes-Griffin CM, Compston P (2015) The effect of processing temperature and placement rate on the short beam strength of carbon fibre–PEEK manufactured using a laser tape placement process. Compos A Appl Sci Manuf 78:274–283
25. Oromiehie E, Prusty BG, Compston P, Rajan G (2019) Automated fibre placement based composite structures: review on the defects, impacts and inspections techniques. Compos Struct 224:110987

26. Landry A (ed) (2015) The needs for automation in composite design and manufacturing. In: The second international symposium on automated composites manufacturing. Montreal, Canada
27. Béland S (1990) High performance thermoplastic resins and their composites: Noyes Data Corp
28. August Z, Ostrander G, Michasiow J, Hauber D (2014) Recent development in automated fibre placement of thermoplastic composites. SAMPE 50(2):30–37
29. Jonsson M, Eklund D, Järneteg A, Åkermo M, Sjölander J (eds) (2015) Automated manufacturing of an integrated pre-preg structure. In: The second international symposium on automated composites manufacturing. Montreal, Canada
30. Di Francesco M, Giddings P, Potter K (eds) (2015) On the layup of convex corners using automated fibre placement: an evaluation method. In: the second international symposium on automated composites manufacturing. Montreal, Canada
31. Girdauskaite L, Krzywinski S, Schmidt-Eisenlohr C, Krings M (eds) (2015) Introduction of automated 3d vacuum buildup in the composite manufacturing chain. In: The second international symposium on automated composites manufacturing. Montreal, Canada
32. Quddus M, Brux A, Larregain B, Galarneau Y (eds) (2015) A study to determine the influence of robotic lamination programs on the precision of automated fiber placement through statistical comparisons. In: The second international symposium on automated composites manufacturing. Montreal, Canada
33. Serubibi A, Hazell PJ, Escobedo JP et al (2023) Fibre-metal laminate structures: high-velocity impact, penetration, and blast loading–a review. Compos A Appl Sci Manuf 173:107674
34. Serubibi A, Hazell PJ, Escobedo JP, Wang H, Oromiehie E, Prusty GB (2021) Analysis of AFP manufactured fibre metal laminate structures under impact loading. Engineers Australia, BARTON, ACT
35. Maung PT, Prusty BG, Oromiehie E, Phillips AW, St John NA (2022) Design and manufacture of a shape-adaptive full-scale composite hydrofoil using automated fibre placement. Int J Adv Manuf Technol 123(11):4093–4108
36. Air A, Shamsuddoha M, Oromiehie E, Prusty BG (2023) Development of an automated fibre placement-based hybrid composite wheel for a solar-powered car. Int J Adv Manuf Technol 125(9):4083–4097
37. Maung PT, Prusty BG, Donough MJ, Oromiehie E, Phillips AW, St John NA (2023) Automated manufacture of optimised shape-adaptive composite hydrofoils with curvilinear fibre paths for improved bend-twist performance. Mar Struct 87:103327
38. Garg DP, Zikry MA, Anderson GL (2001) Current and potential future research activities in adaptive structures: an ARO perspective. Smart Mater Struct 10(4):610–623
39. Chung DDL (2010) Composite materials: science and applications, 2nd edn. Springer, London, United Kingdom, p 371
40. Bannister M (2001) Challenges for composites into the next millennium—a reinforcement perspective. Compos A Appl Sci Manuf 32(7):901–910
41. Spenser J (2006) Boeing technologies developed for commercial jetliners are now being integrated into some military products. Boeing Frontiers Online
42. Efficiency and reliability: Airbus (2023). Available from: https://www.airbus.com/en/products-services/commercial-aircraft/passenger-aircraft/a380
43. Balageas D (2006) Introduction to structural health monitoring. Wiley Online Library
44. Prusty BG, Oromiehie E, Rajan G (2016) Introduction to composite materials and smart structures. In: Iniewski K (ed) Structural health monitoring of composite structures using fiber optic methods. Devices, Circuits, and Systems. CRC Press, New York, pp 1–19
45. Elmar W, Bernhard J (2014) Composites market report. The European GRP market (AVK) TgCmC
46. Prepregs: Composites One (2017). Available from: http://www.compositesone.com/product/prepreg/
47. What are prepregs? Fibre Glast Development Corporation (n.d.) [Available from: http://www.fibreglast.com/product/about-prepregs/Learning_Center

48. Daniel IM, Ishai O (2006) Engineering mechanics of composite materials, 2nd edn. Oxford University Press, New York
49. Thermosets: Polymers International Australia (2014) [Available from: http://polymers.com.au/thermosets/
50. Common Thermoplastics and Thermoseting and there uses: United Kingdom: Stephens Plastic Mouldings (n.d.) cited 2015. Available from: http://www.stephensinjectionmoulding.co.uk/thermoplastics/
51. Chang IY, Lees JK (1988) Recent development in thermoplastic composites: a review of matrix systems and processing methods. J Thermoplast Compos Mater 1(3):277–296
52. Muzzy JD, Kays AO (2004) Thermoplastic versus thermosetting structural composites. Polymer Compos 5(3)
53. Zeng J-J, Liang S-D, Li Y-L, Guo Y-C, Shan G-Y (2021) Compressive behavior of FRP-confined elliptical concrete-filled high-strength steel tube columns. Compos Struct 266:113808
54. Gain AK, Oromiehie E, Prusty BG (2022) Nanomechanical characterisation of CF-PEEK composites manufactured using automated fibre placement (AFP). Compos Commun 31:101109
55. Oromiehie E, Gain AK, Donough MJ, Prusty BG (2022) Fracture toughness assessment of CF-PEEK composites consolidated using hot gas torch assisted automated fibre placement. Compos Struct 279:114762
56. Oromiehie E, Gain AK, Prusty BG (2021) Processing parameter optimisation for automated fibre placement (AFP) manufactured thermoplastic composites. Compos Struct 272:114223
57. Arns J-Y, Oromiehie E, Arns C, Prusty BG (2021) Micro-CT analysis of process-induced defects in composite laminates using AFP. Mater Manuf Process 1–10
58. Oromiehie E, Garbe U, Prusty BG (2019) Porosity analysis of carbon fibre reinforced polymer laminates manufactured using automated fibre placement. Compos Mater
59. Matti FN, Oromiehie E, Mashiri FR, Prusty BG (2022) Strengthening of steel beams with thermoplastic CFRP overwrapping using automated fibre placement. In: Proceedings of the 3rd International Conference on Structural Engineering Research (iCSER 2022), 20–22 November 2022, Sydney, Australia, pp 107–114
60. Online SA (2016) Steel structures, AS 1163–2016. SAI Global database 1998
61. Online SA (1998) Steel structures, AS 4100–1998. SAI Global database 1998
62. OneSteel Market Mills (2004) Cold formed structural hollow sections and profiles, 4th edn